Inorganic Chemistry
Article

Inorg. Chem. **2010**, *49*, 6967–6973 **6967**
DOI: 10.1021/ic1003758

Mechanism of Accumulation and Incorporation of Organometallic Pd Complexes into the Protein Nanocage of apo-Ferritin

Satoshi Abe,[†] Tatsuo Hikage,[‡] Yoshihito Watanabe,[§] Susumu Kitagawa,[†,∥] and Takafumi Ueno*[,†,⊥]

[†]*Institute for Integrated Cell-Material Sciences* (*iCeMS*), *Funai Center, Kyoto University, Katsura, Nishikyo-ku, Kyoto 615-8510, Japan,* [‡]*High Intensity X-ray Diffraction Laboratory, and* [§]*Research Center for Materials Science, Nagoya University, Nagoya 464-8602, Japan,* [∥]*Department of Synthetic Chemistry and Biological Chemistry, Graduate School of Engineering, Kyoto University, Katsura, Nishikyo-ku, Kyoto 615-8510, Japan, and* [⊥]*PRESTO, Japan Science and Technology Agency* (*JST*), *Honcho, Kawaguchi, Saitama 332-0012, Japan*

Received February 24, 2010

Hybridization of metal complexes and protein scaffolds is an important subject in bioinorganic chemistry and materials science. Efforts to provide non-natural functions to proteins will likely lead to advances in development of catalysts, sensors, and so on. Mechanistic investigations of the process of binding of metal complexes within protein scaffolds and characterization of the resulting coordination structures will help us to design and control coordination structures of metal complexes for construction of hybrid proteins containing metal complexes. In this work, the processes of accumulation and incorporation of organometallic palladium complexes within the cage of the iron storage protein apo-ferritin (apo-Fr) are elucidated by analysis of X-ray crystal structures of apo-Fr and selected mutants thereof, in the presence of the metal complexes. The crystal structure of apo-Fr containing Pd(allyl) (allyl = η^3-C_3H_5) complexes shows that thiolato-bridged dinuclear Pd(allyl) complexes are formed at two binding sites within the cage of apo-Fr. The crystal structures of apo-Fr and its Cys- and His-deletion mutants containing Pd(allyl) complexes indicate that Cys126 accelerates the incorporation of Pd(allyl) complexes into the cage. In addition, Cys48 and Cys126 are essential for accumulation of Pd(allyl) complexes and stabilizing the square planar coordination structure.

Introduction

The processes of hybridization of synthetic metal complexes with protein scaffolds have attracted much attention in bioinorganic chemistry and materials science.[1−4] In particular, organometallic complexes, which have many applications for catalysis and biomaterials, and so on, can provide non-natural functions to proteins.[5−14] A number of reports have described protein composites containing organometallic complexes. For example, highly enantioselective reactions catalyzed by rhodium and ruthenium complexes have been carried out in the avidin and the mutant cavities.[5,15,16] Ruthenium arene complexes and cisplatin have been incorporated into protein scaffolds in investigations of the interactions between metal drugs and proteins.[11,17,18] Although

*To whom correspondence should be addressed. E-mail: taka@icems.kyoto-u.ac.jp. Phone: 81-75-383-2812. Fax: 81-75-383-2812.

(1) Lu, Y.; Yeung, N.; Sieracki, N.; Marshall, N. M. *Nature* **2009**, *460*, 855–862.
(2) Ueno, T.; Abe, S.; Yokoi, N.; Watanabe, Y. *Coord. Chem. Rev.* **2007**, *251*, 2717–2731.
(3) Steinreiber, J.; Ward, T. R. *Coord. Chem. Rev.* **2008**, *252*, 751–766.
(4) Uchida, M.; Klem, M. T.; Allen, M.; Suci, P.; Flenniken, M.; Gillitzer, E.; Varpness, Z.; Liepold, L. O.; Young, M.; Douglas, T. *Adv. Mater.* **2007**, *19*, 1025–1042.
(5) Wilson, M. E.; Whitesides, G. M. *J. Am. Chem. Soc.* **1978**, *100*, 306–307.
(6) Hwang, H. J.; Carey, J. R.; Brower, E. T.; Gengenbach, A. J.; Abramite, J. A.; Lu, Y. *J. Am. Chem. Soc.* **2005**, *127*, 15356–15357.
(7) Collot, J.; Gradinaru, J.; Humbert, N.; Skander, M.; Zocchi, A.; Ward, T. R. *J. Am. Chem. Soc.* **2003**, *125*, 9030–9031.
(8) Satake, Y.; Abe, S.; Okazaki, S.; Ban, N.; Hikage, T.; Ueno, T.; Nakajima, H.; Suzuki, A.; Yamane, T.; Nishiyama, H.; Watanabe, Y. *Organometallics* **2007**, *26*, 4904–4908.
(9) Ronconi, L.; Sadler, P. J. *Coord. Chem. Rev.* **2007**, *251*, 1633–1648.
(10) Bruijnincx, P. C. A.; Sadler, P. J. *Curr. Opin. Chem. Biol.* **2008**, *12*, 197–206.
(11) Debreczeni, J. E.; Bullock, A. N.; Atilla, G. E.; Williams, D. S.; Bregman, H.; Knapp, S.; Meggers, E. *Angew. Chem., Int. Ed.* **2006**, *45*, 1580–1585.
(12) Ohashi, M.; Koshiyama, T.; Ueno, T.; Yanase, M.; Fujii, H.; Watanabe, Y. *Angew. Chem., Int. Ed.* **2003**, *42*, 1005–1008.
(13) Ueno, T.; Koshiyama, T.; Ohashi, M.; Kondo, K.; Kono, M.; Suzuki, A.; Yamane, T.; Watanabe, Y. *J. Am. Chem. Soc.* **2005**, *127*, 6556–6562.
(14) Ueno, T.; Koshiyama, T.; Abe, S.; Yokoi, N.; Ohashi, M.; Nakajima, H.; Watanabe, Y. *J. Organomet. Chem.* **2007**, *692*, 142–147.
(15) Letondor, C.; Humbert, N.; Ward, T. R. *Proc. Natl. Acad. Sci. U.S.A.* **2005**, *102*, 4683–4687.
(16) Letondor, C.; Pordea, A.; Humbert, N.; Ivanova, A.; Mazurek, S.; Novic, M.; Ward, T. R. *J. Am. Chem. Soc.* **2006**, *128*, 8320–8328.
(17) McNae, I. W.; Fishburne, K.; Habtemariam, A.; Hunter, T. M.; Melchart, M.; Wang, F. Y.; Walkinshaw, M. D.; Sadler, P. J. *Chem. Commun.* **2004**, 1786–1787.
(18) Yang, Z.; Wang, X. Y.; Diao, H. J.; Zhang, J. F.; Li, H. Y.; Sun, H. Z.; Guo, Z. J. *Chem. Commun.* **2007**, 3453–3455.

Published on Web 06/29/2010

several crystal structures of organometallic complex−protein composites have been reported, the incorporation process and binding mechanism of metal complexes accumulated within protein scaffolds remains obscure.[8,11,17,19,20] Mechanistic investigations are expected to provide guidelines for rational design of coordination structures of organometallic complexes to improve their reactivities within protein scaffolds. A combination of X-ray structural analysis and site-directed mutagenesis is expected to provide the means for elucidating fundamental roles of amino acid residues on the binding of metal complexes.[21,22]

Ferritin (Fr) is an iron storage protein composed of 24 subunits which form a self-assembled spherical cage with an interior space 8 nm in diameter. Apo-Fr has been utilized as a protein container for the deposition of metal nanoparticles and for the incorporation of metal complexes.[23−33] It is known that metal ions and metal complexes are incorporated into the cage of apo-Fr by penetration through the 3-fold channel.[34−36] Many studies have employed X-ray crystallographic analysis of apo-Fr containing metal ions in attempts to clarify protein-metal ion interactions on the interior surface of apo-Frs.[22,32,36−38] A crystal structure of Human H-chain ferritin (HuHF) containing Zn(II) ions indicates that the metal ions are bound to His and Cys at the outer channel of the 3-fold axis and are expected to be sequentially translocated to Glu and Asp at the inner channel of the 3-fold axis.[36] We have recently elucidated the accumulation mechanism of metal ions in the apo-Fr cage by means of crystal structure analysis of apo-Fr containing various quantities of Pd(II) ions.[22] Pd(II) ions are accumulated at the specific binding sites with several binding modes on the interior surface of apo-Fr.

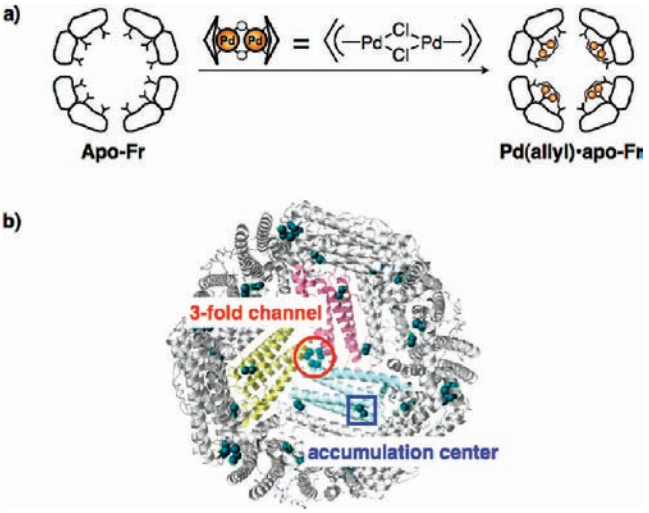

Figure 1. (a) Preparation of **Pd(allyl)·apo-rHLFr**. (b) The crystal structure of **100-Pd(allyl)·apo-rHLFr**. Pd(allyl) complexes are located at the binding sites, 3-fold channel, and accumulation center on the interior surface. The **100-Pd(allyl)·apo-rHLFr** structure is taken from PDB ID 2ZG7. The Pd atoms are indicated as sphere models colored greenish blue.

In this paper, we describe crystal structure analyses of apo-recombinant horse L-ferritin (apo-rHLFr), and Cys- and His-deletion mutants containing Pd(allyl) complexes. Apo-rHLFr is useful to determine coordination structures of many metal ions incorporated in the cage because the L-ferritin subunit lacks the metal binding site of the diiron catalytic center, and crystal structures of apo-rHLFr and the corresponding composites have been reported at high resolution.[29,39] We have recently demonstrated the preparation of apo-rHLFr immobilizing Pd(allyl) complexes for promotion of a Suzuki coupling reaction (Figure 1a).[29] The crystal structure of the composite of apo-rHLFr containing 96 Pd(allyl) complexes indicates that the formation of dinuclear Pd(allyl) complexes proceeds via ligation of the thiol group of Cys residues as bridging ligands as well as ligation of His imidazole, Glu45, and water molecules at the accumulation center and the 3-fold channel (Figure 1b and Figure 2a, 2b, and 2c).[29] Here, we have determined the crystal structures of apo-rHLFr and selected mutants (apo-C48A-rHLFr, apo-C126A-rHLFr, apo-H49A-rHLFr, and apo-H114A-rHLFr) containing Pd(allyl) complexes to clarify the incorporation and accumulation processes of organometallic Pd complexes at the 3-fold channel and the accumulation center where the Cys and His residues are expected to play crucial roles. The analysis of these structures is expected to provide insights into the design of the interior surface of apo-rHLFr to optimize control of coordination structures of metal complexes for future development of biocatalysts, biosensors, metal-drugs, and new inorganic materials.

(19) Creus, M.; Pordea, A.; Rossel, T.; Sardo, A.; Letondor, C.; Ivanova, A.; Le Trong, I.; Stenkamp, R. E.; Ward, T. R. *Angew. Chem., Int. Ed.* **2008**, *47*, 1400–1404.
(20) Rutten, L.; Wieczorek, B.; Mannie, J.; Kruithof, C. A.; Dijkstra, H. P.; Egmond, M. R.; Lutz, M.; Gebbink, R.; Gros, P.; van Koten, G. *Chem.—Eur. J.* **2009**, *15*, 4270–4280.
(21) Ueno, T.; Abe, S.; Koshiyama, T.; Ohki, T.; Hikage, T.; Watanabe, Y. *Chem.—Eur. J.* **2010**, *16*, 2730–2740.
(22) Ueno, T.; Abe, M.; Hirata, K.; Abe, S.; Suzuki, M.; Shimizu, N.; Yamamoto, M.; Takata, M.; Watanabe, Y. *J. Am. Chem. Soc.* **2009**, *131*, 5094–5100.
(23) d'Estaintot, B. L.; Paolo, S.; Granier, T.; Gallois, B.; Chevalier, J. M.; Precigoux, G.; Levi, S.; Arosio, P. *J. Mol. Biol.* **2004**, *340*, 277–293.
(24) Shenton, W.; Pum, D.; Sleytr, U. B.; Mann, S. *Nature* **1997**, *389*, 585–587.
(25) Douglas, T.; Dickson, D. P. E.; Betteridge, S.; Charnock, J.; Garner, C. D.; Mann, S. *Science* **1995**, *269*, 54–57.
(26) Iwahori, K.; Yoshizawa, K.; Muraoka, M.; Yamashita, I. *Inorg. Chem.* **2005**, *44*, 6393–6400.
(27) Kramer, R. M.; Li, C.; Carter, D. C.; Stone, M. O.; Naik, R. R. *J. Am. Chem. Soc.* **2004**, *126*, 13282–13286.
(28) Aime, S.; Frullano, L.; Crich, S. G. *Angew. Chem., Int. Ed.* **2002**, *41*, 1017.
(29) Abe, S.; Niemeyer, J.; Abe, M.; Takezawa, Y.; Ueno, T.; Hikage, T.; Erker, G.; Watanabe, Y. *J. Am. Chem. Soc.* **2008**, *130*, 10512–10514.
(30) Niemeyer, J.; Abe, S.; Hikage, T.; Ueno, T.; Erker, G.; Watanabe, Y. *Chem. Commun.* **2008**, 6519–6521.
(31) Abe, S.; Hirata, K.; Ueno, T.; Morino, K.; Shimizu, N.; Yamamoto, M.; Takata, M.; Yashima, E.; Watanabe, Y. *J. Am. Chem. Soc.* **2009**, *131*, 6958–6960.
(32) Suzuki, M.; Abe, M.; Ueno, T.; Abe, S.; Goto, T.; Toda, Y.; Akita, T.; Yamadae, Y.; Watanabe, Y. *Chem. Commun.* **2009**, 4871–4873.
(33) Ueno, T.; Suzuki, M.; Goto, T.; Matsumoto, T.; Nagayama, K.; Watanabe, Y. *Angew. Chem., Int. Ed.* **2004**, *43*, 2527–2530.
(34) Levi, S.; Santambrogio, P.; Corsi, B.; Cozzi, A.; Arosio, P. *Biochem. J.* **1996**, *317*, 467–473.
(35) Barnes, C. M.; Theil, E. C.; Raymond, K. N. *Proc. Natl. Acad. Sci. U.S.A.* **2002**, *99*, 5195–5200.
(36) Toussaint, L.; Bertrand, L.; Hue, L.; Crichton, R. R.; Declercq, J. P. *J. Mol. Biol.* **2007**, *365*, 440–452.
(37) Granier, T.; Comberton, G.; Gallois, B.; d'Estaintot, B. L.; Dautant, A.; Crichton, R. R.; Precigoux, G. *Proteins: Struct. Funct. Bioinform.* **1998**, *31*, 477–485.
(38) Butts, C. A.; Swift, J.; Kang, S. G.; Di Costanzo, L.; Christianson, D. W.; Saven, J. G.; Dmochowski, I. J. *Biochemistry* **2008**, *47*, 12729–12739.
(39) Hempstead, P. D.; Yewdall, S. J.; Fernie, A. R.; Lawson, D. M.; Artymiuk, P. J.; Rice, D. W.; Ford, G. C.; Harrison, P. M. *J. Mol. Biol.* **1997**, *268*, 424–448.

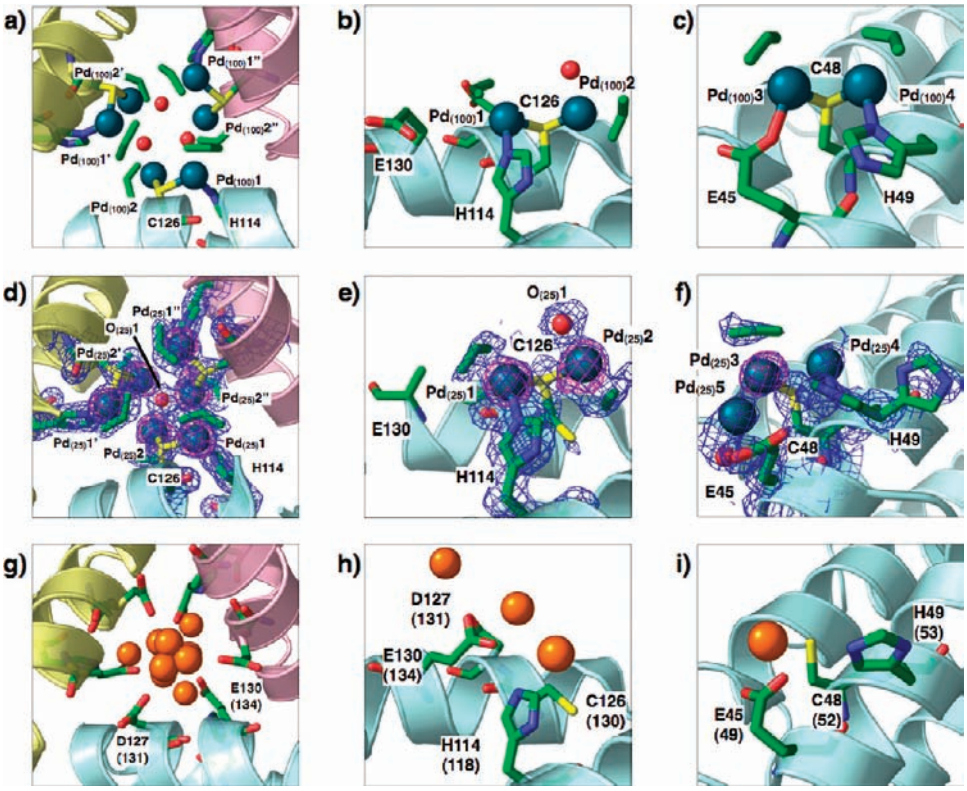

Figure 2. Crystal structures of **100-Pd(allyl)·apo-rHLFr** (a−c), **25-Pd(allyl)·apo-rHLFr** (d−f), and Pd-free·apo-rHLFr (g-i). Close views of 3-fold symmetric channel (a, d, and g), 3-fold channel structure of monomer unit (b, e, and h), and accumulation centers (c, f, and i). The **100-Pd(allyl)·apo-rHLFr** and Pd-free·apo-rHLFr structures are taken from PDB IDs 2ZG7 and 1AEW, respectively.[29,39] The Pd and Cd atoms are indicated as sphere models colored greenish blue and orange, respectively. The O atoms of water molecules are shown as red sphere. The anomalous difference Fourier maps at 4.0 σ indicate that the positions of palladium atoms which are shown in magenta. The selected $2|F_o| - |F_c|$ electron density maps at 1.0 σ are shown in blue.

Table 1. Quantitative Analysis of Pd Atoms in **Pd(allyl)·apo-rHLFrs**

reaction conditions [Pd(allyl)]$_2$/ [apo-rHLFr]	Pd atoms determined by ICP-OES and BCA assay	Pd binding sites determined by crystal structural analysis
25:1 (apo-rHLFr)	54 ± 4 (2.2)[b]	120(5)[a]
50:1 (apo-rHLFr)	106 ± 1 (4.4)[b]	
100:1 (apo-rHLFr)	103 ± 1 (4.3)[a,b]	96(4)[a,b]
100:1 (apo-H114A-rHLFr)	78 ± 6 (3.2)[a,b]	72(3)[a,b]
100:1 (apo-C126A-rHLFr)	37 ± 4 (1.5)[a,b]	48(2)[b]
100:1 (apo-C48A-rHLFr)	62.5 ± 1.5 (2.6)[b]	48(2)[b]
100:1 (apo-H49A-rHLFr)	99 ± 4 (4.1)[a,b]	96(4)[a,b]

[a] The results are taken from ref 29. [b] The number of Pd atoms/subunit is shown in parentheses.

Results and Discussion

Preparation and Crystallization of Pd(allyl)·apo-rHLFrs and Pd(allyl)·apo-rHLFr mutants. The composites of apo-rHLFr were prepared by reaction with 25 and 50 equiv of [Pd(allyl)Cl]$_2$ (**25-Pd(allyl)·apo-rHLFr and 50-Pd(allyl)·apo-rHLFr**). An acetonitrile solution of [Pd(allyl)Cl]$_2$ was added to the aqueous solution of apo-rHLFr (10 μM, 5 mL in 50 mM Tris/HCl (pH 8.0), 0.15 M NaCl). The reaction mixture (9% acetonitrile) was stirred for 1 h at 25 °C as reported previously,[29] followed by dialysis against 0.15 M NaCl aqueous solution for 6 h. The composite was purified with a size exclusion column (ÄKTA design, Superdex G-200) to remove the unbound Pd(allyl) complexes. The number of Pd atoms in the cage of apo-Fr was determined by Pd atoms and apo-rHLFr concentrations obtained from inductively coupled plasma-optical emission spectrometry (ICP-OES) measurements and a bicinchonic acid (BCA) assay, respectively.[29,33] The results show that **25-Pd(allyl)·apo-rHLFr** and **50-Pd(allyl)·apo-rHLFr** contain 54 ± 4 and 106 ± 1 Pd atoms per apo-rHLFr, respectively (Table 1), and all Pd(allyl) complexes reacted with apo-rHLFr have been accumulated in the cage of apo-rHLFr. The quantity of Pd complexes in **50-Pd(allyl)·apo-rHLFr** is almost identical to that of **100-Pd(allyl)·apo-rHLFr** (103 ± 1).[29] These results indicate that this quantity represents the maximum amount of Pd(allyl) complexes that can be incorporated into the cage of apo-rHLFr.

The crystal structure of **100-Pd(allyl)·apo-rHLFr** shows that there are two binding sites for Pd(allyl) complexes at the 3-fold channel and at the accumulation center (Figure 1b).[29] The dinuclear Pd(allyl) structures are retained by the bridged ligand of Cys126 and Cys48 at the binding sites (Figure 2b and 2c). The Cys residues appear to be essential for deposition of Pd(allyl) complexes within the cage. Thus, to clarify the role of the residues, Cys-deleted mutants, apo-C126A-rHLFr and apo-C48A-rHLFr, were prepared. When 100 equiv of [Pd(allyl)Cl]$_2$ was added to each of the two mutants under the same conditions used for apo-rHLFr, the subsequent quantitative analysis of Pd atoms indicated that **100-Pd(allyl)·apo-C126A-rHLFr** and **100-Pd(allyl)·apo-C48A-rHLFr** contained 37 ± 4 and 62.5 ± 1.5 Pd atoms per the mutants, respectively (Table 1). All composites were crystallized using the hanging-drop vapor diffusion method under the same conditions used for **100-Pd(allyl)·apo-rHLFr**.[29]

Table 2. Summary of X-ray Data and Refinement Statistics for **Pd(allyl)·apo-rHLFrs**

	25-Pd(allyl)·apo-rHLFr	100-Pd(allyl)·apo-C126A-rHLFr	100-Pd(allyl)·apo-C48A-rHLFr
	Data Collection Statistics		
X-ray wavelength, Å	0.5080	1.0000	0.5080
space group	*F*432	*F*432	*F*432
unit cell, Å	181.520	181.984	182.433
resolution range	30−1.58	30−1.66	30−1.85
(outer shell) (Å)	1.64−1.58	1.72−1.66	1.92−1.85
total observations	799, 972	666,224	511,560
unique reflections	35,634	31,026	22,730
completeness (%)[a]	99.9 (100)	100 (100)	100 (100)
R_{merge} (%)[a,b]	8.3 (28.5)	4.9 (17.5)	9.4 (27.2)
$I/\sigma(I)$ [a]	75.3 (16.8)	87.6 (20.1)	69.1(19.5)
	Refinement Statistics		
resolution (Å)	25.17−1.58	27.76−1.66	25.55−1.85
no. reflections working set/test set	33,824/1,786	29,411/1,563	21,557/1,162
R-factor (%)[c]	19.2	18.1	17.7
R_{free} (%)[d]	21.2	19.5	20.5
	Final Model		
no. of residues	172 (1−130, 132−173)	172 (2−173)	171 (2−172)
no. of water molecules	183	184	153
no. of Pd complexes and Pd atoms	5	2	2
no. of Cd atoms	1	3	3
no. of Sulfate ions	1	1	1
no. of ethylene glycol	5	7	7
rms deviation from ideality			
bonds (Å)	0.016	0.009	0.011
angle (deg)	1.314	1.074	1.232
Ramachandran plot (%)[e]			
most favored	93.5	93.6	94.9
allowed	6.5	6.4	5.1

[a] Values in parentheses are for the highest resolution shell. [b] $R_{merge} = \sum|I - \langle I\rangle|/\sum I$, where I is the integrated intensity of a given reflection. [c] $R = \sum||F_o| - |F_c||/\sum|F_o|$, where F_o and F_c are the observed and calculated structure factor amplitudes, respectively. [d] R_{free}: an R factor calculated on a partial set that is not used in the refinement of the structure. [e] Ramachandran plot parameters were calculated using *PROCHECK*.

Crystal Structure of 25-Pd(allyl)·apo-rHLFr. To elucidate the process of accumulation of Pd(allyl) complexes on the interior surface of apo-rHLFr, the crystal structure of **25-Pd(allyl)·apo-rHLFr** was refined at 1.58 Å resolution (Table 2). The root-mean-square deviations (rmsd) of the Cα atoms of **25-Pd(allyl)·apo-rHLFr** from those of apo-rHLFr and **100-Pd(allyl)·apo-rHLFr** are 0.49 and 0.27, respectively.[29,39] These values indicate that the whole assembly structure of apo-rHLFr is preserved after incorporation of Pd(allyl) complexes. We have distinguished the Pd atoms from Cd atoms, which are essential for the crystallization of the composites, by using anomalous Fourier difference maps in which data sets from a single crystal were collected at 0.5080 and 0.4632 Å of peak wavelength of Pd and Cd atoms, respectively.[22] The anomalous Fourier difference maps show that two Pd atoms ($Pd_{(25)}1$ and $Pd_{(25)}2$) and three Pd atoms ($Pd_{(25)}3$, $Pd_{(25)}4$, and $Pd_{(25)}5$) are observed at the 3-fold channel and at the accumulation center, respectively (Figure 2d−2f). The total number of Pd binding sites observed in the crystal structure (120 Pd atoms/apo-rHLFr) is greater than the number of Pd atoms estimated by ICP-OES and BCA method (54 Pd atoms/apo-rHLFr) (Table 1). The coordination structures of the Pd atoms at the 3-fold channel are almost identical to those of **100-Pd(allyl)·apo-rHLFr** except for the coordination of a water molecule ($O_{(25)}1$) and the double conformation of Cys126 (Figure 2a, 2b, 2d, and 2e). The water molecule is located on the 3-fold axis and interacts with three Pd(allyl) complexes ($Pd_{(25)}2$, $Pd_{(25)}2'$, and $Pd_{(25)}2''$) with a $Pd_{(25)}2-O_{(25)}1$ distance of 2.27 Å, although a single water molecule is coordinated to the $Pd_{(100)}2$ at each subunit in **100-Pd(allyl)·apo-rHLFr**.[29] The sulfur atom of Cys126 (which has alternative conformations) is coordinated to $Pd_{(25)}1$ and $Pd_{(25)}2$ as a bridging ligand to form a dinuclear coordination structure with $Pd_{(25)}1$-S^{γ}_{Cys126} and $Pd_{(25)}2$-S^{γ}_{Cys126} distances of 2.27 and 2.40 Å, respectively (Figure 2e). The other conformer of Cys126 is free from coordination with Pd(allyl) complexes and represents the same conformation observed in the structure of Pd-free·apo-rHLFr (Figure 2h).[39]

Three anomalous maps corresponding to Pd atoms are observed at the accumulation center in **25-Pd(allyl)·apo-rHLFr** (Figure 2f). $Pd_{(25)}3$ and $Pd_{(25)}4$ are coordinated by S^{γ}_{Cys48} and N^{δ}_{His49}, respectively, with $Pd_{(25)}3$-S^{γ}_{Cys48} and $Pd_{(25)}4$-N^{δ}_{His49} distances of 2.45 and 1.90 Å, respectively. The distance of $Pd_{(25)}4$ with S^{γ}_{Cys48} (3.18 Å) is longer than the distance of $Pd_{(100)}4$ with S^{γ}_{Cys48} of **100-Pd(allyl)·apo-rHLFr** (2.31 Å) (Figure 2c and 2f). $Pd_{(25)}3$ and $Pd_{(25)}4$ independently exist as mononuclear complexes at the accumulation center in **25-Pd(allyl)·apo-rHLFr**. The side chain of His49 adopts two conformations which are bound and unbound to $Pd_{(25)}4$ as shown in Figure 2f. The side chain of Glu45 is oriented in a conformation opposite $Pd_{(25)}3$, while Glu45 is bound to a $Pd_{(100)}3$ atom in **100-Pd(allyl)·apo-rHLFr** for stabilization of dinuclear complexes. The anomalous difference maps reveal an additional Pd(allyl) binding site, $Pd_{(25)}5$, located adjacent

to $Pd_{(25)}3$. The $Pd_{(25)}5$ atom only coordinates to a single water molecule with distance of 2.23 Å and has no apparent interactions with any amino acid residues. The $Pd_{(25)}3-Pd_{(25)}5$ distance of 2.37 Å is too short for formation of a Pd−Pd bond.[40] It is expected that $Pd_{(25)}3$ and $Pd_{(25)}5$ are not bound to the same subunit at the same time. The structures of the allyl ligand of $Pd_{(25)}4$ and $Pd_{(25)}5$ were not determined because of significantly decreased density corresponding to the allyl ligand in the vicinity of $Pd_{(25)}4$ and $Pd_{(25)}5$ (Figure 2f). The occupancies of the Pd atoms are below 0.5. These results indicate that Pd(allyl) complexes are able to take several coordination modes at the accumulation center of **25-Pd(allyl)·apo-rHLFr**. Therefore, there is a difference in the number of Pd atoms of estimated by quantitative analysis (54 ± 4) from that of the crystal structure (120) because all of the Pd atoms in **25-Pd(allyl)·apo-rHLFr** are superimposed on the single subunit as reported for Pd^{II}·apo-rHLFr.[22]

Crystal Structures of Cys-Deletion Mutants Containing Pd(allyl) Complexes. To elucidate the role of the Cys residue in coordination of Pd(allyl) complexes at each binding site, crystal structures of the Cys-deletion mutants containing Pd(allyl) complexes, **100-Pd(allyl)·apo-C126A-rHLFr** and **100-Pd(allyl)·apo-C48A-rHLFr** were refined at 1.66 and 1.85 Å, respectively. The X-ray data and refinement statistics are listed in Table 2. The root-mean-square deviations (rmsd) of the Cα atoms of **100-Pd(allyl)·apo-C126A-rHLFr** and **100-Pd(allyl)·apo-C48A-rHLFr** from that of **100-Pd(allyl)·apo-rHLFr** are 0.21 and 0.16, respectively, indicating that the whole structures of apo-ferritin mutants are not affected by the deletion of these Cys residues. The number of Pd(allyl) complexes observed by crystal structure analysis of **100-Pd(allyl)·apo-C126A-rHLFr** (48 Pd atoms/apo-C126A-rHLFr) is half of that of **100-Pd(allyl)·apo-rHLFr** (96 Pd atoms/apo-rHLFr). **100-Pd(allyl)·apo-C126A-rHLFr** has no Pd(allyl) complexes located at the 3-fold axis channel because of the lack of Cys126. Alternatively, two Cd ions, which are necessary for crystallization, are bound to O^{ε} atom of Glu130 and O^{δ} atom of Asp127 at the 3-fold channel as observed in Pd-free·apo-rHLFr (Figure 3a).[37,39] Examination of **100-Pd(allyl)·apo-C126A-rHLFr** indicates that it has a coordination structure of a dinuclear Pd(allyl) complex at the accumulation center which is similar to that of **100-Pd(allyl)·apo-rHLFr** with the exception that Glu45 adopts two conformations (Figure 2c and 3b).

The crystal structure of **100-Pd(allyl)·apo-C48A-rHLFr** shows that 6 anomalous maps corresponding to Pd atoms are located at the 3-fold axis of the symmetric channel (Figure 3c). The coordination structure of the dinuclear Pd(allyl) complex (PdB1 and PdB2) is the same as that of **100-Pd(allyl)·apo-rHLFr** although the structure of the allyl ligand in the vicinity of PdB2 could not be determined because of the low density of the allyl ligand (Figure 2a and 3c). There are no anomalous maps of Pd atoms at the accumulation center because of the deletion of Cys48. The imidazole ring of His49 adopts two conformations bound and unbound to a Cd ion (Figure 3d). The quantity of Pd atoms in **100-Pd(allyl)·apo-C48Ar-HLFr** estimated by ICP and BCA (62.5 ± 1.5) is larger than that observed in the X-ray crystal structure (48). This suggests that several Pd complexes are located at nonspecific binding sites within the cage.

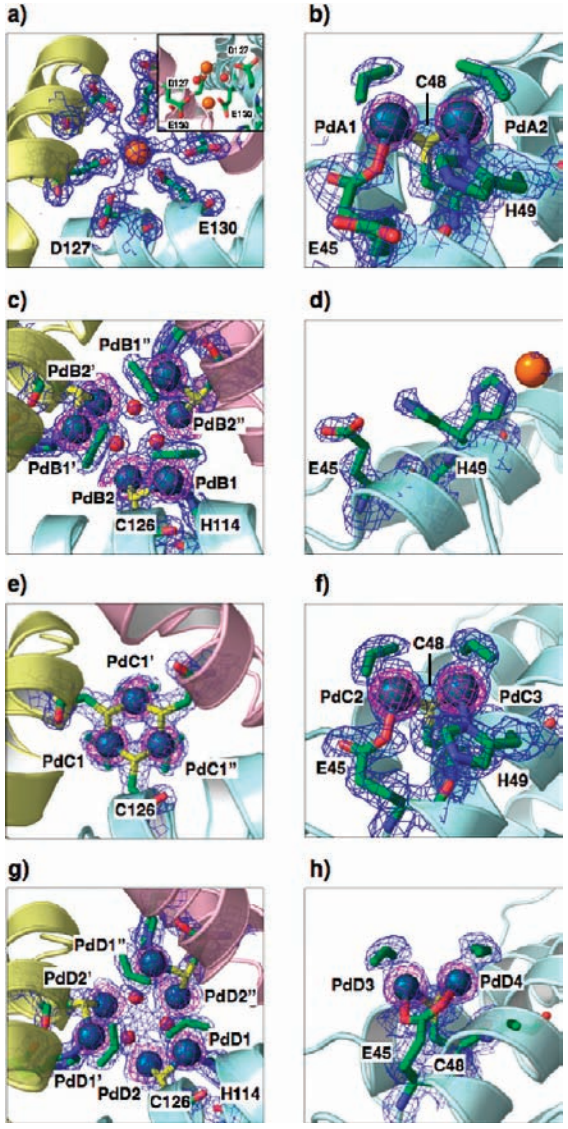

Figure 3. Crystal structures of 3-fold symmetric channels and accumulation centers of **100-Pd(allyl)·apo-C126A-rHLFr** (a and b), **100-Pd(allyl)·apo-C48A-rHLFr** (c and d), **100-Pd(allyl)·apo-H114A-rHLFr** (e and f), **100-Pd(allyl)·apo-H49A-rHLFr** (g and h), respectively. The inset of a is perpendicular to the 3-fold asymmetric channel of **100-Pd(allyl)·apo-C126A-rHLFr**. The **100-Pd(allyl)·apo-H114A-rHLFr** and **100-Pd(allyl)·apo-H49A-rHLFr** structures are taken from PDB IDs 2ZG9 and 2ZG8, respectively.[29] The Pd and Cd atoms are indicated as greenish and orange spheres, respectively. The anomalous difference Fourier maps at 4.0 σ indicate the positions of palladium atoms which are shown in magenta. The selected $2|F_o| - |F_c|$ electron density maps at 1.0 σ are shown in blue.

Incorporation Mechanism of Pd(allyl) Complexes at the 3-Fold Channel. The 3-fold channel is known as the major point of entry of metal ions into the apo-rHLFr cage.[34−36] The crystal structures of apo-rHLFr containing metal ions show that the metal ions bind to His114 (118), Cys126 (130), Asp127 (131), and Glu130 (134), which are highly conserved residues in most of Frs, at the 3-fold channel (where the residue numbers in parentheses are the analogous residues of Human H−Fr).[36,37] This suggests that the metal ions migrate to the inner cage of apo-Fr with transient interactions with these amino acid residues. The

(40) Burrows, A. D.; Mingos, D. M. P. *Transition Met. Chem.* **1993**, *18*, 129–148.

crystal structure of **25-Pd(allyl)·apo-rHLFr** shows that the three dinuclear Pd(allyl) complexes are coordinated at the 3-fold channel with high occupancies compared to the Pd atoms located at the accumulation center. Thus, Pd(allyl) complexes appear to be incorporated through the 3-fold channel, in turn, bound to the accumulation center because the size of moiety of Pd(allyl) is smaller than that of maltose, which can penetrate through the channels into the ferritin cavity.[41] Cys126 adopts two conformers, one conformer is free from coordination of Pd(allyl) complexes with a similar conformation to that of Pd-free·apo-rHLFr (Figure 2e and 2h).[39] The other conformer serves as a bridging ligand of $Pd_{(25)}1$ and $Pd_{(25)}2$ as found in **100-Pd(allyl)·apo-rHLFr**. It is expected that the capture of Pd(allyl) complexes is promoted by the conformational changes of the side chain of Cys126 at the channel. The side chain of Glu130 of **100-Pd(allyl)·apo-rHLFr** is deviated from the position in Pd-free·apo-rHLFr because of the steric hindrance of $Pd_{(25)}1$(allyl) complex bound to His114 and Cys126 (Figure 2b and 2h). The crystal structure of **100-Pd(allyl)·apo-C126A-rHLFr** shows that there are no Pd(allyl) complexes bound to the 3-fold channel as a result of the Cys to Ala mutation. The quantity of Pd atoms in **100-Pd(allyl)·apo-C126A-rHLFr** (37 ± 4) determined by quantitative analysis is slightly smaller than the amount observed in the crystal structure (48) (Table 1). The apo-C48A-rHLFr mutant contains 62.5 ± 1.5 Pd complexes. This number is greater than the observed quantity of Pd(allyl) complexes in the crystal structure of **100-Pd(allyl)·apo-C48A-rHLFr** (48). The different quantity observed for the Cys-deleted mutants suggests that Cys126 is a critical residue for formation of Pd(allyl) dinuclear complexes and that this residue plays a role in facilitating the uptake of the Pd complexes at the 3-fold channel. Cys126 is also expected to influence the uptake of other metal ions such as Pd(II), Cd(II), and Fe(II).[22,34,37,42]

When His114, which binds to Pd(allyl) complexes in **100-Pd(allyl)·apo-rHLFr**, is deleted, a thiolato-bridged trinuclear Pd(allyl) complex is formed by coordination of three S^{γ} atoms of Cys126 residues at the 3-fold channel.[29] The deletion of His114 causes a 2.4 Å shift of the Cα position of Cys126 toward the center of the 3-fold channel to maintain the square-planar geometry with an allyl ligand and the three S^{γ} atoms (Figure 3e). The coordination structures of PdC2 and PdC3 at the accumulation center are identical to that of **100-Pd(allyl)·apo-rHLFr** (Figure 3f). The quantity of Pd atoms in the apo-H114AFr estimated by ICP and BCA measurements (78 ± 6) is essentially identical to the number of Pd atoms observed in the crystal structure (72) (Table 1). The results indicate that His114 plays a role in stabilizing the Pd(allyl) dinuclear structure at the 3-fold channel in apo-rHLFr.

Binding Mechanism of Pd(allyl) Complexes at the Accumulation Center. At the accumulation center of **100-Pd(allyl)·apo-rHLFr**, a Pd(allyl) dinuclear structure is maintained by the thiolato-bridged ligation of Cys48, which is found only in HLFr, and the supporting coordination of His49 and Glu45 (Figure 1c).[29] In Pd-free·apo-rHLFr, Cd(II) ion is located in the vicinity of Cys48 and Glu45. The orientation of the imidazole ring of His49 in Pd-free·apo-rHLFr is different from those of **25-Pd(allyl)·apo-rHLFr** and **100-Pd(allyl)·apo-rHLFr** (Figure 2c, 2f and 2i). The crystal structure of **25-Pd(allyl)·apo-rHLFr** shows that 120 Pd binding sites (a greater number than the quantity determined by quantitative analyses (54 ± 4)) were identified with low occupancies (Table 1). The occupancies of the $Pd_{(25)}3$, $Pd_{(25)}4$, and $Pd_{(25)}5$ atoms at the accumulation center are estimated to be lower than the occupancies of the $Pd_{(25)}1$ and $Pd_{(25)}2$ atoms at the 3-fold channels. At the initial stage of Pd(allyl) binding, the Pd(allyl) complexes appear to be captured at the positions of $Pd_{(25)}3$, $Pd_{(25)}4$, and $Pd_{(25)}5$. The $Pd_{(25)}3$ and $Pd_{(25)}4$ atoms are coordinated by the S^{γ} atom of Cys48 and the N^{ε} atom of His49, respectively, as mononuclear complexes. As the number of Pd(allyl) complexes within the apo-rHLFr cage increases, the occupancies of $Pd_{(25)}3$ and $Pd_{(25)}4$ also increase, and $Pd_{(25)}5$ disappears. Finally, a thiolato-bridged Pd(allyl) dinuclear complex is formed by coordination of Cys48, His49, and Glu45 as shown in Figure 1c.

The crystal structure of **100-Pd(allyl)·apo-C48A-rHLFr** shows that there are no Pd(allyl) complexes at the accumulation center. This indicates that Cys48 is a crucial residue for formation of a dinuclear Pd(allyl) complex. His49 of **25-Pd(allyl)·apo-rHLFr** and **100-Pd(allyl)·apo-C48A-rHLFr** has two conformers, indicating that the side chain of His49 is highly flexible. The imidazole ring of His49 is expected to adopt several conformations which enable it to adapt to various metal coordination geometries. When metal ions such as Pd(II) and Au(III) ions are bound to the accumulation center, the conformation of His49 is dramatically altered by the coordination of the metal ions.[22,32] The crystal structure of **100-Pd(allyl)·apo-H49A-rHLFr** shows that the quantity of Pd atoms observed in the cage is 96. This is the same quantity observed in **100-Pd(allyl)·apo-rHLFr**. **100-Pd(allyl)·apo-H49A-rHLFr** has thiolato-carboxylato dinuclear Pd complexes which are formed by ligation of Cys48 and Glu45 at the accumulation center as a result of an alternative conformation of the side chain of Glu45 (Figure 3h).[29] These results suggest that the conformational changes of His49 and Glu45 contribute to the stability of the square planar thiolato-bridged dinuclear Pd(allyl) complexes.

In summary, these substitution experiments of Cys and His show that (1) Cys126 accelerates the incorporation of metal complexes by inducing a conformational change at the 3-fold channel, and (2) Cys48 is essential for formation of dinuclear Pd(allyl) complexes at the accumulation center. The quantity of Pd(allyl) complexes bound in the interior surface of apo-rHLFr depends on the quantity of Cys residues at the appropriate sites. Apo-rHLFr is thus able to bind 96 Pd(allyl) complexes because apo-Fr has a total of 48 Cys residues, which are expected to be needed to maintain the dinuclear Pd(allyl) structures. His and Glu residues which have flexible side chain structures in the vicinity of Cys residues are necessary for stabilization of the dinuclear Pd(allyl) structures. This suggests that introduction of additional Cys residues within the apo-rHLFr cage would promote an increase in the capacity of the cage to accommodate greater quantities of Pd(allyl)

(41) Yang, D. W.; Nagayama, K. *Biochem. J.* **1995**, *307*, 253–256.
(42) Bou-Abdallah, F.; Zhao, G.; Biasiotto, G.; Poli, M.; Arosio, P.; Chasteen, N. D. *J. Am. Chem. Soc.* **2008**, *130*, 17801–17811.

complexes. The coordination structures of Pd(allyl) complexes could be controlled by altering the positions of His and Glu residues on the interior surface of apo-rHLFr.

Experimental Section

Materials. Reagents were purchased from TCI, Wako, Nacalai Tesque, and Sigma-Aldrich and used without further purification. Apo-recombinant L-Fr from horse liver was prepared in NovaBlue competent cells (Novgen) transformed with the expression vector pMK2. Apo-C126A-rHLFr and apo-C48A-rHLFr mutants were prepared using a Stratagene Quikchange MultiSite kit. The culture and purification of the proteins were performed according to a previous literature.[26]

Preparation of Pd(allyl)·apo-rHLFrs. An acetonitle solution of $[Pd(allyl)Cl]_2$ (10 mM) was added to an apo-rHLFr buffer solution (10 μM, 10 mL in 50 mM Tris/HCl pH 8.0, 0.15 M NaCl) and stirred for 1 h at 25 °C. After dialysis against a 0.15 M NaCl aqueous solution, the mixture was purified by gel filtration (Superdex G-200) equilibrated in a 0.15 M NaCl aqueous solution. The number of Pd atoms in Pd(allyl)·apo-rHLFrs were determined by ICP-OES and Bicichonianate (BCA) methods.

Crystallization of Pd(allyl)·apo-rHLFrs. Crystallization of Pd(allyl)·apo-Frs were performed with a hanging drop vapor diffusion method as described in previous reports.[29,37,39] A solution of Pd(allyl)·apo-rHLFr was concentrated to approximately 20 mg mL^{-1}, and the drops were prepared by mixing an equal volume (3 μL) of a protein solution (20 mM Tris/HCl pH8.0, 0.15 M NaCl aq.) and the precipitant solution (1 M $(NH_4)_2SO_4$, 20 mM $CdSO_4$), and equilibrated against the precipitant solution (1 mL) at 20 °C. The crystals were obtained within a day.

X-ray Crystal Analysis. Before the data collection of Pd(allyl)·apo-rHLFr, single crystals were immersed in a precipitant solution containing 30% (w/w) ethylene glycol and subsequently frozen in liquid nitrogen. X-ray diffraction data of **25-Pd(allyl)·apo-rHLFr** and **100-Pd(allyl)·apo-C48A-rHLFr** were collected at 100 K at beamline BL41XU at SPring-8 using X-ray wavelength of 0.5080 Å and 0.4632 Å which represent the peak wavelengths of Pd and Cd X-ray absorption, respectively, to distinguish Pd atoms from Cd atoms which are essential for crystallization. X-ray diffraction data of **100-Pd(allyl)·apo-C126A-rHLFr** was collected at 100 K at beamline BL38B1 at SPring-8 using X-ray wavelength of 1.0 Å. The data were processed with HKL2000 programs in the cubic *F*432 space group. The crystal parameters and data collection statistic are summarized in Table 2.

Refinement. The structures were determined by molecular replacement with MOLREP using an apo-Fr structure (pdb ID: 1DAT) as the initial model. Refinement of the protein structure was performed using REFMAC5[43] in the CCP4 suite. Rebuilding was performed using COOT[44] based on σ weighted ($2F_o - F_c$) and ($F_o - F_c$) electron density maps. About 5% of the observed data were excluded from the refinements and used to calculate the free R (R_{free}) as a monitor of model bias. Water molecules were positioned to fit residual ($F_o - F_c$) density peaks with a lower cutoff of 3σ. The models were subjected to quality analysis during the various refinement stages with omit maps and PROCHECK.[45] The refinement statistics are summarized in Table 2. Residues Ser131 and Asp174 of **25-Pd(allyl)·apo-rHLFr**, Ser1 and Asp174 of **100-Pd(allyl)·apo-C126A-rHLFr**, and Ser1, His173, and Asp174 of **100-Pd(allyl)·apo-C48A-rHLFr** were not decided because of their disordered electron densities. Residues Glu53, Asp127, Glu130, Glu136, and Lys172 of **25-Pd(allyl)·apo-rHLFr**, Lys172 of **100-Pd(allyl)·apo-C126A-rHLFr**, and Glu53, Glu136, and Lys172 of **100-Pd(allyl)·apo-C48A-rHLFr** were replaced to Ala because electron densities of these residues are missing. Atomic coordinates are deposited in the Protein Data Bank under accession numbers 3AF7, 3AF8, and 3AF9 for **25-Pd(allyl)·apo-rHLFr**, **100-Pd(allyl)·apo-C126A-rHLFr**, and **100-Pd(allyl)·apo-C48A-rHLFr**, respectively.

Physical Measurements. Absorption spectra were recorded on a Shimazu UV-2400PC UV−vis spectrometer. The number of Pd atoms in the cage of apo-rHLFr was determined by Pd and apo-Fr concentrations.[29,33] Metal concentrations of **Pd(allyl)·apo-rHLFrs** were determined by using an inductively coupled plasma atomic emission (ICP) spectrometer (Varian ICP-OES Vista-PRO). $PdCl_2$ in 0.1 M HCl (1.01 g/L) was used as calibration standard and $Y(NO_3)_3$ in 0.1 M HNO_3 (1.01 g/L) was applied for an internal standard. Protein concentration of **Pd(allyl)·apo-rHLFrs** were determined by a bicinchonic acid (BCA) assay.

Acknowledgment. We thank members of BL38B1 and BL41XU of SPring-8 for assistance during the diffraction data collection. This work was supported by a grant from the 21st Century- and Global-COE program of Nagoya University for S. A., Grant-in-Aid for Scientific Research (Grant 18685019 for T.U.) and on Priority Areas (Grant 16033226, Chemistry of Coordination Space for Y.W.) from Ministry of Education, Culture, Sports, Science and Technology, Japan, and PRESTO, Japan Science and Technology Agency (JST). Synchrotron radiation experiments were conducted under the approval of 2008A1124 and 2009B1059 at SPring-8.

(43) Murshudov, G. N.; Vagin, A. A.; Dodson, E. J. *Acta Crystallogr., Sect. D* **1997**, *53*, 240–255.
(44) Emsley, P.; Cowtan, K. *Acta Crystallogr., Sect. D* **2004**, *60*, 2126–2132.
(45) Laskowski, R. A.; Macarthur, M. W.; Moss, D. S.; Thornton, J. M. *J. Appl. Crystallogr.* **1993**, *26*, 283–291.